Broadband Photonic RF Channelization Based on Optical Sampling Pulse Shaping

Sitong Wang, Yiwei Sun, Jianping Chen, *Member, IEEE*, and Guiling Wu, *Member, IEEE*

***Abstract*— We propose a photonic radio-frequency (RF) channelization scheme which can slice the frequency spectrum into different subchannels through shaping the optical sampling pulse of each subchannel. An optical pulse shaper, which is composed of two cascaded multi-tap optical pulse shapers, is used in each subchannel to shape the sampling pulse. The principle of proposed scheme is theoretically analyzed, and experimentally verified. Through shaping the sampling pulse, the channel responses with 500 MHz bandwidth and center frequency of 7.5 GHz/ 8.5 GHz are experimentally measured.**

***Index Terms*— Microwave photonics, optical pulse shaping, radio-frequency signal processing.**

I. Introduction

With the development of digital technology, the traditional analog-component-based military radio-frequency (RF) receiver with large size, weight and power (SWaP) is gradually replaced by the digital receiver [1]. Meanwhile, the applications in satellite communications, electronic warfare (EW) and radar system drive the receiver toward higher frequency and wider bandwidth, which has brought a tremendous challenge to the existing analog-to-digital converters (ADCs) [2]. RF channelization, which can slice the spectrum into a bank of narrow channels, is an effective solution to relieve the pressure of the ADCs and provide a high-resolution measurement [3].

Conventional electric channelized receivers utilize a large number of contiguous filters to sort the RF signal by frequency. The complex structure, high energy consumption and the bandwidth limitation of electric devices limit the use of electric channelized receivers in EW applications [4]. Benefiting from the merits of photonics, such as light-weight, high frequency and wide bandwidth, several photonic-assisted RF channelizers have been proposed to break the restriction [2], [5]–[8]. In most of the schemes, the received RF signal is up-converted to the optical domain and split to different subchannels by optical filters [5]–[7]. However, the narrow optical filter is difficult to obtain and the requirement of flattop and steep-edge amplitude response further increase the fabrication difficulty. In [2], the channelizers based on two optical frequency combs avoid the requirement of narrow optical filters, but the number of subchannels is limited by the number of the flat optical frequency combs.

Manuscript received July 2, 2020; revised July 29, 2020; accepted August 10, 2020. Date of publication August 14, 2020; date of current version August 24, 2020. This work was supported in part by the National Natural Science Foundation of China under Grant 61627817 and Grant 61535006. *(Corresponding author: Guiling Wu.)*

The authors are with the State Key Laboratory of Advanced Optical Communication Systems and Networks, Shanghai Jiao Tong University, Shanghai 200240, China (e-mail: wuguiling@sjtu.edu.cn).

Color versions of one or more of the figures in this letter are available online at http://ieeexplore.ieee.org.

Digital Object Identifier 10.1109/LPT.2020.3016677

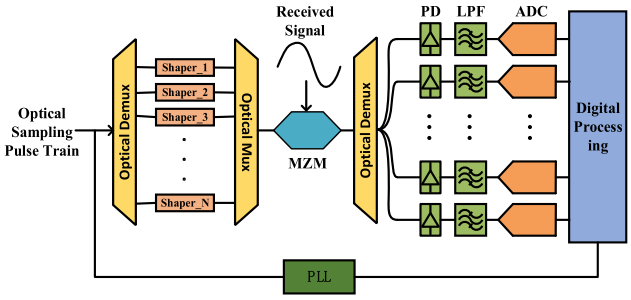

Fig. 1. The proposed photonic channelization scheme. MZM, Mach-Zehnder modulator; PD, photodiode; LPF, low-pass filter; PLL, phase locked loop.

In this letter, based on the principle of simultaneous filtering and digitizing and the structure of photonic analog-to-digital conversion [9]–[11], an optical sampling pulse shaping based channelization scheme is presented. Through shaping the optical sampling pulses of each subchannel, the equivalent amplitude response of each subchannel can be easily designed and flexibly reconfigured to slice the received signal's spectrum. The proposed photonic channelization scheme has no need of narrow optical filters or multiple laser sources, and can realize the spectrum slicing and sampling of the received signal at the same time. Additionally, the response of each subchannel can be adjusted to different center frequencies in near real time according to the requirements of applications. The proposed scheme is theoretically analyzed and experimentally verified.

II. Principle of Operation

Figure 1 illustrates the schematic of the proposed photonic channelization scheme based on optical sampling pulse shaping. The optical sampling pulse train is divided into each subchannel, and shaped by a corresponding optical pulse shaper. The shaped sampling pulse train in each subchannel is converged together by an optical MUX and modulated by the received signal via an electro-optic modulator, which is usually a lithium niobate Mach–Zehnder modulator (MZM). The modulated pulse train is demultiplexed to different subchannels and detected by a corresponding photodiode (PD). The detected electric pulses in each subchannel are then

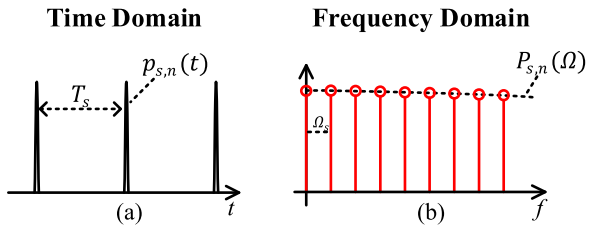

Fig. 2. (a) The schematic of the n-th optical sampling pulse train's temporal shape, (b) The schematic of the n-th optical sampling pulse train's spectrum in the electrical domain.

filtered by an analog low-pass filter (LPF) and quantized by an ADC. The obtained sample in each subchannel is the sampling result of the received signal in the designed frequency channel determined by the shaper in corresponding subchannel.

The temporal shape of the optical sampling pulse train in the n-th channel, shown in Fig. 2(a), can be expressed as

$$p_n(t) = P_{A,n} \sum_{m=-\infty}^{+\infty} p_{s,n}(t - mT_s), \tag{1}$$

where $P_{A,n}$ is the average power of the n-th optical sampling pulse train, $p_{s,n}(t)$ is the temporal shape of the single optical sampling pulse normalized by $P_{A,n}$, and T_s is the repetition period. The corresponding spectrum of the n-th sampling pulse train in the electrical domain, shown in Fig. 2(b), can be expressed as

$$P_n(\Omega) = \frac{2\pi P_{A,n}}{T_s} \sum_{k=-\infty}^{+\infty} P_{s,n}(k\Omega_s)\delta(\Omega - k\Omega_s), \tag{2}$$

where $P_{s,n}(\Omega)$ is the spectrum of $p_{s,n}(t)$, $\delta(\Omega)$ is the Dirac function, and $\Omega_s = 2\pi / T_s$. Eq. (2) indicates that the envelope of $P_n(\Omega)$ (the black dashed line in Fig. 2(b)) is proportional to the spectrum of the single sampling pulse $P_{s,n}(\Omega)$. Corresponding to the narrow full width at half maxima (FWHM) of $p_{s,n}(t)$ and the periodicity of $p_n(t)$, $P_n(\Omega)$ is discrete and its envelope has a quite large bandwidth.

According to [12], the equivalent impulse response of the n-th channel, $h_{A,n}(t)$, is determined by the shape of the n-th sampling pulse train and can be expressed as

$$h_{A,n}(t) = -0.5\alpha h_M(t) * [h_{E,n}(t) p_n(-t)], \tag{3}$$

where α and $h_M(t)$ are respectively the attenuation factor and the impulse response of the intensity modulation, $h_{E,n}(t)$ is the back-end impulse response accounting from the photodector (PD) to the ADC on the n-th channel, and $*$ represents the convolution operation. The effect of the modulator is equivalent to a cascade filter with a relatively large bandwidth, and can be investigated independently. The corresponding equivalent response of the n-th channel can be expressed as

$$\begin{aligned} H_{A,n}(\Omega) &\propto H_{E,n}(\Omega) * P_n(-\Omega) \\ &\propto \sum_{k=-\infty}^{+\infty} P_{s,n}(k\Omega_s) H_{E,n}(\Omega + k\Omega_s), \end{aligned} \tag{4}$$

where $H_{E,n}(\Omega)$ is the spectrum of $h_{E,n}(t)$. According to Eq. (4), the equivalent response of the n-th channel can

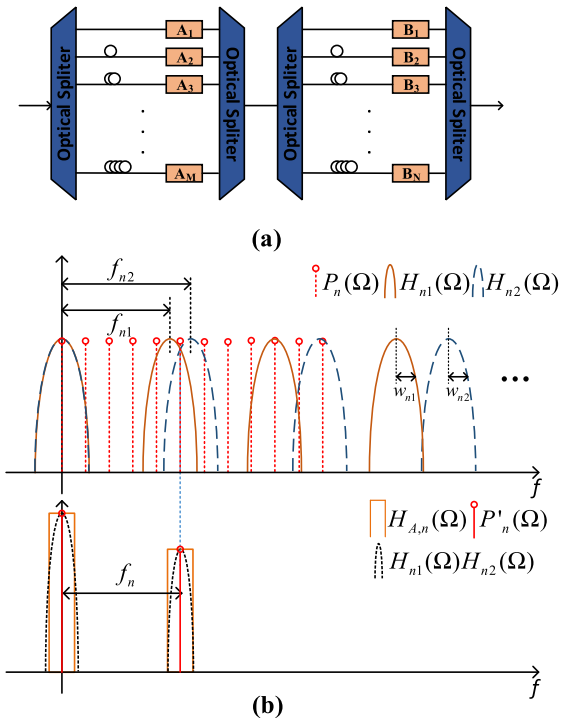

Fig. 3. (a) The schematic of the optical pulse shaper, (b) The schematic of the optical pulse shapers' response and the shaped optical sampling pulse train's spectrum in the electrical domain.

be sliced as a separate passband through shaping the n-th sampling pulse train to filter a single frequency component out from $P_n(\Omega)$. The filtered frequency component determines the passband's center frequency and Ω_s determines the minimum interval of adjacent channels' center frequencies. The filtering response accounting from the PD to the ADC, $H_{E,n}(\Omega)$, determines the passband's bandwidth, flatness and roll-off factor.

Fig. 3(a) shows an optical pulse shaper composed of two cascaded multi-tap optical pulse shapers for the shaping of n-th sampling pulse train, and the shaped sampling pulse train $p_n'(t)$ can be expressed as

$$\begin{cases} p_n'(t) = p_n(t) * h_{n1}(t) * h_{n2}(t) \\ h_{n1}(t) = \sum_{i=1}^{M} A_i \delta(t - iT_{n1}) \\ h_{n2}(t) = \sum_{i=1}^{N} B_i \delta(t - iT_{n2}) \end{cases}, \tag{5}$$

where $h_{n1}(t)$ and $h_{n2}(t)$ are the impulse response of the two multi-tap optical pulse shapers, A_i and B_i are their respective taps' weights, T_{n1} and T_{n2} are their respective delay between the adjacent taps. In the frequency domain, the spectrum of $p_n'(t)$ can be expressed as

$$P_n'(\Omega) = P_n(\Omega) H_{n1}(\Omega) H_{n2}(\Omega), \tag{6}$$

where the functions denoted by an upper-case letter are the Fourier transform of the functions expressed by the corresponding lower-case letter.

As shown in Fig. 3(b), the multi-tap optical pulse shapers can be easily designed and adjusted by altering A_i,

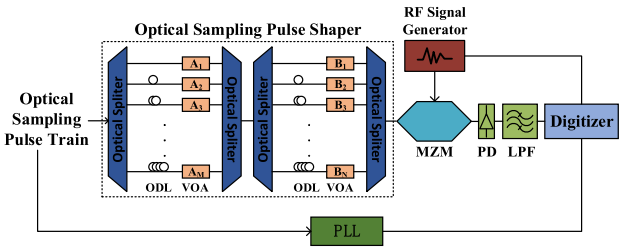

Fig. 4. Experiment setup of the proposed photonic channelization scheme. ODL, optical delay line; VOA, variable optical attenuator.

B_i and T_{n1}, T_{n2}. The periods of the two multi-tap optical pulse shapers' amplitude response are $f_{n1}= 1/T_{n1}$, and $f_{n2}= 1/T_{n2}$, respectively. The passband cut-off frequencies of the responses, w_{n1} and w_{n2}, are determined by the taps' weights A_i, B_i, respectively.

In order to filter a single frequency component out from the sampling pulse train's spectrum, the periods and the passband cut-off frequencies of the two multi-tap optical pulse shapers' responses are set as

$$\begin{cases} f_{n1} < f_n < f_{n2} \\ f_n < f_{n1} + w_{n1} < f_n + \frac{1}{T_s} \\ f_n - \frac{1}{T_s} < f_{n2} - w_{n2} < f_n \end{cases}, \tag{7}$$

where f_n is the frequency component needs to be filtered out in the n-th subchannel. It is worth noting that the frequency component f_n is always a multiple of $1/T_s$, and w_{n1}, w_{n2} are usually far less than f_{n1}, f_{n2}. If the condition shown in Eq. (7) is satisfied, the two multi-tap optical pulse shapers' passbands is only overlapped at near DC and f_n, and the $P_n(\Omega)$'s frequency components located at DC and f_n can be filtered out as shown in Fig. 3(b). Although there is always a frequency component located at DC, it does not matter when a high-pass filter is applied to avoid the low frequency interference in the received signal.

According to Eq. (4), the n-th channel response is a passband located at f_n, and its passband width is twice as the back-end's bandwidth. Combining multiple subchannels with different center frequencies through wavelength-division multiplexing, a photonic channelized receiver can be realized. Additionally, a time-division multiplexing photonic channelized receiver can also be realized with only one channel and tunable optical pulse shapers.

III. Experimental Setup and Results

The basic principle of the scheme is validated using a single channel system, considering different subchannels have the same structure and are independent each other. Figure 4 shows the experiment setup of the proposed photonic channelization scheme. The optical pulse train from a mode-locked laser (MLL) with a 250 MHz repetition rate is multiplied to 500 MHz by an optical time division multiplexing module (OTDM) to obtain the sampling pulse train. The optical sampling pulse train is shaped by the optical pulse shaper, which is composed of two multi-tap optical pulse shapers. The shaped sampling pulse train is modulated by the RF signals from a microwave signal generator (Rohde & Schwarz, SMF100A) in a 20 GHz MZM biased at quadrature with a half-wave voltage of ~4.6V. The frequency of the generated RF signal can be controlled by the back-end digitizer for the measurement of the system's response. The power level of the RF input is set at 0 dBm to avoid the MZM nonlinearity. The modulated optical pulse is converted to electronic pulses by a PD with ~500MHz bandwidth. The electronic pulses are filtered by an LPF with 250 MHz bandwidth, and sampled a digitizer with a bandwidth of 650 MHz and an ENOB of 9.0 (Keysight, M9703A). The synchronizing signal is fed into a phase-locked circuit to generate the triggers and clocks for the digitizer.

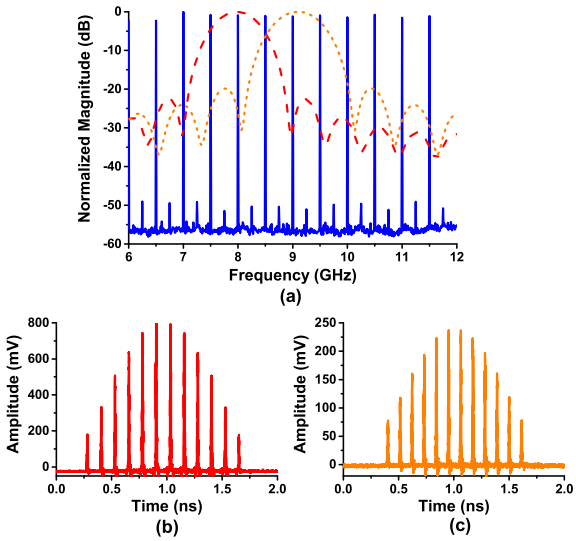

Fig. 5. (a) The measured spectrum of the sampling pulse train (blue solid line) and the amplitude response of the two multi-tap optical pulse shapers (red dashed line and orange short-dashed line). (b) The response of the first multi-tap pulse shaper with tap interval of 125 ps. (c) The response of the second multi-tap pulse shaper with tap interval of ~109.9 ps.

The measured spectrum of the 500 MHz sampling pulse train in the range of 6 GHz to 12GHz is shown in Fig. 5(a) (the blue solid line). One can see that the spectrum is a discrete sequence with the period of 500 MHz and its envelope has a quite large bandwidth as discussed above.

The responses of the two multi-tap optical pulse shapers to a single optical sampling pulse are detected by a 50 GHz PD, then measured and shown in Figs. 5(b) and 5(c), respectively. Both the two shapers have 12 taps and are designed as 11-order rectangular digital filters. In the two shapers, the delay between the adjacent taps are respectively set as ~125 ps and ~109.9 ps, which are corresponding to the response periods of 8 GHz and 9.1 GHz. The delay errors between the adjacent taps are less than 4 ps. The tap's weights of the two shapers are altered to make their passband cut-off frequency are both ~600 MHz. The amplitude responses of the two multi-tap optical pulse shapers in the range of 6 GHz to 12GHz are respectively calculated and shown in Fig. 5(a) (the red dashed line and the orange short-dashed line). The spectrum of the shaped sampling pulse train and the channel amplitude response are measured and shown in Fig. 6. One can see that the single frequency component of the sampling pulse

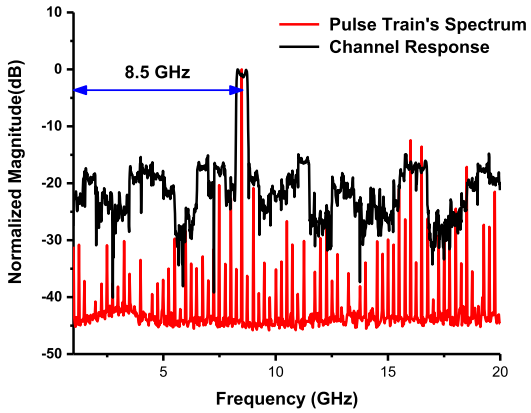

Fig. 6. The measured spectrum of the shaped sampling pulse train and the measured channel's amplitude response with the center frequency of 8.5 GHz.

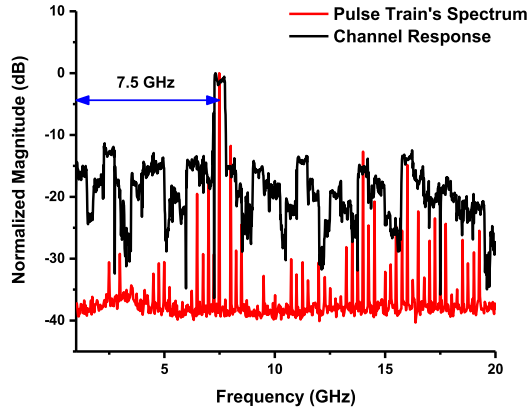

Fig. 7. The measured spectrum of the shaped sampling pulse train and the measured channel's amplitude response with the center frequency of 7.5 GHz.

train's spectrum, which is located at 8.5 GHz, is filtered out by the two multi-tap pulse shapers. The channel response is the shifted replica of the LPF's response, whose center frequency is 8.5 GHz and bandwidth is 500 MHz. The measured results are well consistent with the analyses above, and one subchannel of the proposed photonic channelization scheme is experimentally realized.

To verify the tunability of the proposed photonic channelization scheme, we alter the center frequency of the channel's response by slightly adjusted the second multi-tap pulse shaper. The first shaper's parameters are unchanged, whose response period and passband cut-off frequency are still 8 GHz and ∼600 MHz. In the second shaper, the delay between the adjacent taps is set as 144.9 ps, which is corresponding to the response period of 6.9 GHz. The tap's weights of the second multi-tap pulse shaper are also altered to make its passband cut-off frequency is ∼600 MHz. The spectrum of the shaped pulse train and the channel amplitude response with the adjusted shaper are measured and shown in Fig. 7. One can see that the single frequency component of the sampling pulse train's spectrum, which is located at 7.5 GHz, is filtered out by the multi-tap pulse shapers. The channel response is another shifted replica of the LPF's response, whose center frequency is 7.5 GHz and bandwidth is 500 MHz. It is verified that the center frequency of the channel response can be adjusted through designing and altering the optical pulse shapers as digital filters easily. It worth noting that through increasing the number of multi-tap optical pulse shapers' taps, the shapers' stop-band rejection ratio and the system's out-of-band rejection can be improved.

IV. Conclusion

In conclusion, we present a photonic RF channelization scheme, which can simultaneously realize the spectrum slicing and sampling of the received signal. Through shaping the optical sampling pulse train by a reconfigurable optical pulse shaper, which is implemented by two cascaded multi-tap optical pulse shapers in each channel, we can filter out the wanted single frequency component besides DC. The response of each channel is a narrow passband, whose center frequency is determined by the filtered frequency component's location and bandwidth is determined by the back-end bandwidth. The proposed scheme is theoretically analyzed and experimentally verified. The channel responses with bandwidth of 500 MHz, center frequency of 7.5 GHz/ 8.5 GHz are experimentally measured.

References

[1] D. Gupta *et al.*, "Digital channelizing radio frequency receiver," *IEEE Trans. Appl. Supercond.*, vol. 17, no. 2, pp. 430–437, Jun. 2007.
[2] X. Xie *et al.*, "Broadband photonic RF channelization based on coherent optical frequency combs and I/Q demodulators," *IEEE Photon. J.*, vol. 4, no. 4, pp. 1196–1202, Aug. 2012.
[3] X. Zou, B. Lu, W. Pan, L. Yan, A. Stöhr, and J. Yao, "Photonics for microwave measurements," *Laser Photon. Rev.*, vol. 10, no. 5, pp. 711–734, Sep. 2016.
[4] G. W. Anderson, D. C. Webb, A. E. Spezio, and J. N. Lee, "Advanced channelization for RF, microwave, and millimeterwave applications," *Proc. IEEE*, vol. 79, no. 3, pp. 355–388, Mar. 1991.
[5] X. Zou, W. Pan, B. Luo, and L. Yan, "Photonic approach for multiple-frequency-component measurement using spectrally sliced incoherent source," *Opt. Lett.*, vol. 35, no. 3, pp. 438–440, Feb. 2010.
[6] X. Xie *et al.*, "Broadband photonic radio-frequency channelization based on a 39-GHz optical frequency comb," *IEEE Photon. Technol. Lett.*, vol. 24, no. 8, pp. 661–663, Apr. 15, 2012.
[7] C.-S. Bres *et al.*, "Parametric photonic channelized RF receiver," *IEEE Photon. Technol. Lett.*, vol. 23, no. 6, pp. 344–346, Mar. 15, 2011.
[8] R. Li, H. Chen, Y. Yu, M. Chen, S. Yang, and S. Xie, "Multiple-frequency measurement based on serial photonic channelization using optical wavelength scanning," *Opt. Lett.*, vol. 38, no. 22, pp. 4781–4784, 2013.
[9] F. Su, G. Wu, and J. Chen, "Photonic analog-to-digital conversion with equivalent analog prefiltering by shaping sampling pulses," *Opt. Lett.*, vol. 41, no. 12, pp. 2779–2782, 2016.
[10] S. Wang, G. Wu, F. Su, and J. Chen, "Simultaneous microwave photonic analog-to-digital conversion and digital filtering," *IEEE Photon. Technol. Lett.*, vol. 30, no. 4, pp. 343–346, Feb. 15, 2018.
[11] S. Wang, G. Wu, Y. Su, and J. Chen, "Principle of integrated filtering and digitizing based on periodic signal multiplying," *Opt. Lett.*, vol. 44, no. 7, pp. 1766–1769, 2019.
[12] F. Su, G. Wu, L. Ye, R. Liu, X. Xue, and J. Chen, "Effects of the photonic sampling pulse width and the photodetection bandwidth on the channel response of photonic ADCs," *Opt. Express*, vol. 24, no. 2, pp. 924–934, 2016.